Journal of Magnetism and Magnetic Materials 444 (2017) 161–167

Contents lists available at ScienceDirect

Journal of Magnetism and Magnetic Materials

journal homepage: www.elsevier.com/locate/jmmm

Research articles

Rheological analysis of magnetite added carbonyl iron based magnetorheological fluid

Ehsan Esmaeilnezhad [a], Hyoung Jin Choi [b,*], Mahin Schaffie [a,c], Mostafa Gholizadeh [d], Mohammad Ranjbar [a,e], Seung Hyuk Kwon [b]

[a] Department of Petroleum Engineering, Shahid Bahonar University of Kerman, Kerman, Iran
[b] Department of Polymer Science and Engineering, Inha University, Incheon 402-751, South Korea
[c] Department of Chemical Engineering, Shahid Bahonar University of Kerman, Kerman, Iran
[d] Department of Chemistry, Ferdowsi University of Mashhad, Mashhad 91779-1436, Iran
[e] Department of Mining Engineering, Shahid Bahonar University of Kerman, Kerman, Iran

ARTICLE INFO

Article history:
Received 30 June 2017
Received in revised form 2 August 2017
Accepted 8 August 2017
Available online 9 August 2017

Keywords:
Carbonyl Iron
Magnetite
Magnetorheological fluid
Additive

ABSTRACT

The addition of additives to soft-magnetic carbonyl iron (CI)-based magnetorheological (MR) suspensions is a popular method for solving the intrinsic sedimentation problem. In this study, synthesized magnetite nanoparticles were added to a CI suspension and its enhanced MR properties were investigated using a rotational rheometer. Based on an analysis of the variance, two models were introduced to assess the yield stress and shear viscosity in terms of the CI concentration, additive concentration, and magnetic field strength. The validation of the model was proven statistically through a supplementary experiment. The shear stress of the CI-based MR fluid versus the shear rate could be predicted properly using the proposed models.

1. Introduction

Magnetorheological (MR) smart fluids, which have reversible and tunable ability to transform from a liquid-like to a solid-like structure under an applied magnetic field [1–3], as well as MR elastomers [4], have potential industrial applications, such as designed dampers, clutches, sensors, and polishing devices [5,6]. They are generally made from a mineral oil [7] or silicone oil [8] containing nano- [9] to micron-sized [10] magnetic particles. Among the different types of magnetic particles, such as carbonyl iron (CI) [11], iron oxide (magnetite [12] and maghemite [13]) and alloys, CI particles, owing to their high saturation magnetic property, are used mainly for fabricating MR fluids [14]. On the other hand, the high density difference between CI particles and oil medium [15] results in poor dispersion stability, which impedes CI-based MR fluid applications [16]. Therefore, many types of additives, such as microcrystalline cellulose [17], carbon nanotubes [18], silica [19], laponite [20], graphene oxide [21], have been introduced to solve this problem. The cost of the CI particles is relatively high [22], which is an impediment for the wide commercialization of CI-based MR fluids. Therefore, having a MR fluid with optimal amount of CI would be ideal, especially in industries where cost is a major consideration. In some cases, however, a certain yield stress or shear viscosity at a fixed magnetic field will be needed and making a MR fluid reach this goal using trial and error methods is difficult. Therefore, the aim of this study was to develop a model to predict the MR response of a CI particle-based MR fluid through routine studies of a magnetic additive system in a CI suspension. The MR properties were examined using oscillatory and rational tests. This is the first study to analyze statistically the relationship among various experimental factors that affect the MR response. The analysis of variance technique was used to determine the relationship among the causative factors.

2. Experimental

2.1. Materials

Carbonyl iron (CI) particles with an average size of 7 μm and a density of 7.79 g/cm^3 (standard CM grade, BASF, Germany) as a dispersed phase and silicone oil (density: 0.97 g/cm^3, kinematic viscosity: 1000 cS, Shin-Etsu Co., Ltd. Korea) as a continuous phase were adopted. Fe_3O_4 (magnetite) nano-particles were synthesized based mainly on a previously reported method [23] with a slight modification, in which 1 mmol of $C_6H_5Na_3O_7{\cdot}2H_2O$

* Corresponding author.
E-mail address: hjchoi@inha.ac.kr (H. Jin Choi).

http://dx.doi.org/10.1016/j.jmmm.2017.08.023
0304-8853/

(Sigma-Aldrich Co., Ltd. USA), 2 mmol of $NaNO_3$ (Daejung Chemical & Metals CO., Ltd. Korea), and 4 mmol of NaOH (Merck Co., Ltd. Germany) were dissolved in 19 mL of deionized water and heated to 100 °C. Subsequently, 1 mL of 2 M $FeSO_4{\cdot}7H_2O$ (Yukuri Pure Chemicals CO., Ltd, Japan) was then added rapidly. The entire mixture was kept constant for one hour for the chemical reaction. The resulting brown precipitate was separated by a magnet and washed several times with water. Synthesized magnetite was then added to the CI-based suspension at specified weight percentage and mixed well by mechanical stirring using a vortex (IKA-Genius 3) and sonicator (HSt-Power Sonic 401) to produce the magnetite-added, CI-based MR suspension.

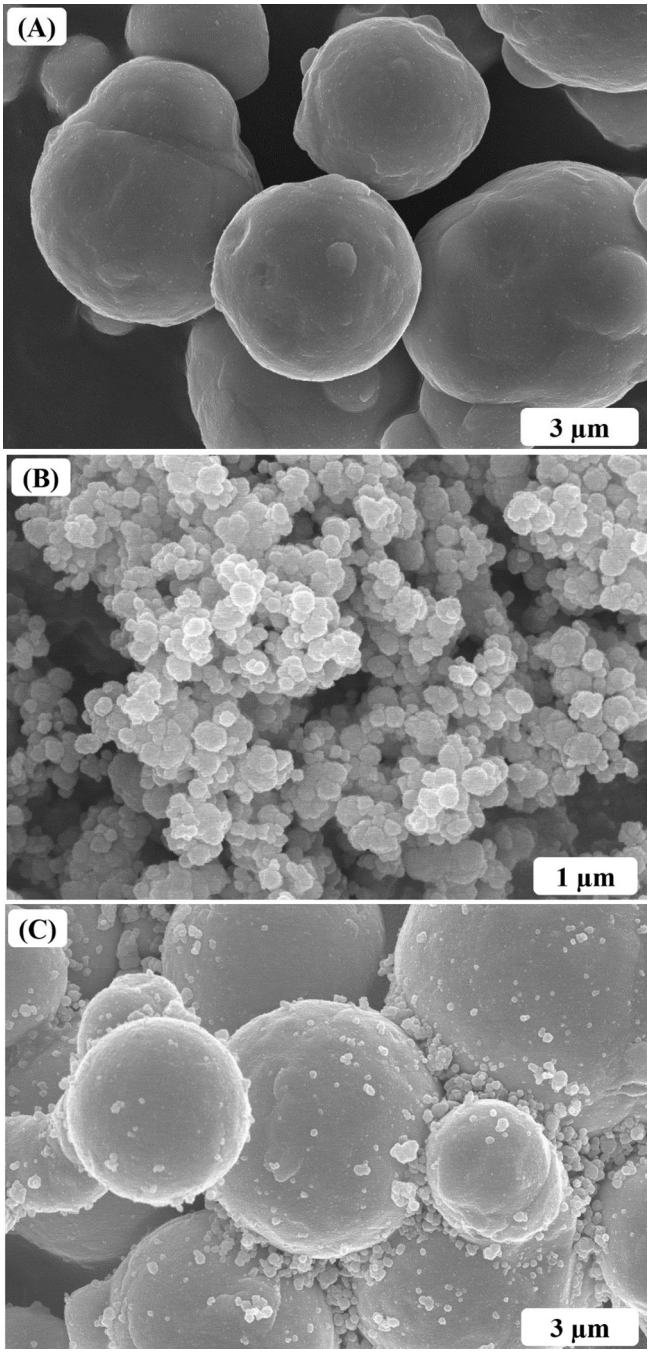

Fig. 1. SEM images of (A) Pure CI, (B) magnetite and (C) CI/Magnetite mixture.

2.2. Characterization

The surface morphologies of the CI, magnetite, and CI/magnetite particles were observed by scanning electron microscopy (SEM, S-4300, Hitachi, Japan). To examine the MR characteristics of the sample, a rotational rheometer (Physica MCR 300, Anton Paar, Germany) equipped with a magnetic field supplier and a 25-mm parallel plate, which generated a homogeneous magnetic field perpendicular to the orientation of the shear rate, was used. All measurements were taken at room temperature (~25 °C).

3. Results and discussion

3.1. MR properties

Initially, the effects of the magnetite additive on the CI-based MR fluid was studied. Two MR fluids with different additive fractions (0 wt% and 0.5 wt% magnetite) at a fixed weight fraction of CI particles (30 wt%) dispersed in silicone oil were prepared. SEM images of CI, magnetite, and CI/magnetite were taken to observe the morphology. Pure CI (Fig. 1(a)) had a smooth surface with a spherical shape and magnetite had a spherical shape with a 100 nm size (Fig. 1(b)). In contrast, the addition of magnetite led to a slightly irregular shape (Fig. 1(c)) due to the magnetite attached to the surface of CI. Nano-sized magnetite particles can fill the gaps among the CI particles and it is anticipated that the MR response of CI/magnetite increases along with improved dispersion stability because of its ability to reduce the sedimentation rate.

A controlled shear rate (CSR) mode under different magnetic field strengths, ranging from 0 to 343 KA/m, was attempted to investigate the MR characteristics of the flow curve. The application of a magnetic field affects the flow behavior of a suspension and its shear stress increases dramatically with increasing magnetic field strength (Fig. 2) as a result of the robust column formation via powerful dipole-dipole interplay between the abutted magnetic particles. The nano-sized magnetite particles can remain on the surface of CI particles and change the free distance among the CI particles. Under an applied magnetic field, magnetite particles can boost the contact among the neighboring CI particle. In the absence of a magnetic field, a slight difference between the curves of the above two mentioned suspensions was detected due to an increase in hydrodynamic volume. In the entire shear rate domain, a wide plateau region was observed under an applied magnetic

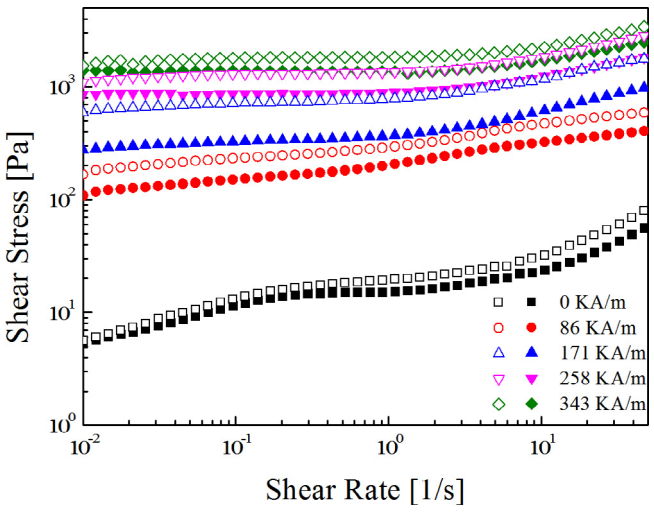

Fig. 2. Shear stress versus shear rate of pure CI (30%wt, closed) and CI/Magnetite (30%wt CI and 0.5%wt magnetite, open) under applying different magnetic field strength.

Table 1
Parameters values of pure CI (30%wt) and CI/Magnetite (30%wt CI and 0.5%wt magnetite) using Bingham, Herschel-Bulkley and Casson model.

Particles	MF Strength (KA/m)	Herschel-Bulkley model parameter				Bingham model parameter			Casson model parameter		
		τ_0	k	n	Adj. R-Square	τ_0	η	Adj. R-Square	τ_0	η_∞	Adj. R-Square
CI	86	50.4	161.92	0.21	0.99	194.3	3.90	0.69	167.2	1.12	0.87
	171	283.4	97.9	0.51	0.99	373.6	11.33	0.90	309.8	3.84	0.98
	258	829.3	97.24	0.59	0.98	920.2	16.71	0.93	814.9	4.03	0.99
	343	1326	86.74	0.65	0.98	1407	19.08	0.93	1283	3.68	0.97
CI/Magnetitle	86	126.9	179.7	0.25	0.99	285.7	5.79	0.73	246.2	1.65	0.90
	171	592.4	229.02	0.4	0.98	800.3	16.38	0.82	693.2	4.52	0.95
	258	1171	214.5	0.51	0.98	1370	24.53	0.88	1210	6.01	0.98
	343	1695	140.3	0.63	0.98	1825	28.01	0.93	1646	5.95	0.98

field. Based on these rheological outputs, an attempt was made to fit the flow curves using the Bingham fluid model as follows [24]:

$$\tau = \tau_y + \eta_0\dot{\gamma}, \quad \tau \geqslant \tau_y \tag{1}$$
$$\dot{\gamma} = 0 \quad \tau < \tau_y$$

where τ_y and τ are the yield stress and shear stress, respectively, and η_0 is the shear viscosity. The following Herschel-Bulkley model was also applied [17]:

$$\tau = \tau_y + K\dot{\gamma}^n \tag{2}$$

where n is the flow behavior index and K is the consistency coefficient. The following Casson model was also considered [25]:

$$\tau^{1/2} = \tau_y^{1/2} + \eta_\infty^{1/2}\dot{\gamma}^{1/2} \tag{3}$$

where η_∞ is a shear viscosity of suspension at an infinite shear rate. The parameters of the above three models are summarized in Table 1. Regarding to Adj. R-Square value, the results could be fitted with Casson and Herschel-Bulkley model better than the Bingham model, particularly in case of the CI/magnetite-based MR fluid.

Furthermore, the yield stress also increased with increasing magnetic field strength and the dynamic yield stress (τ_y) was dependent on the magnetic field strength (H) as follows [26]:

$$\tau_y \propto H^\alpha \tag{4}$$

Fig. 3 shows that the dynamic yield stress was enhanced for both CI and CI/magnetite-based MR fluids with an applied magnetic field strength, and the calculated slope was 1.5, which is reasonable regarding the weight percentage of CI in the suspension [27]. γ

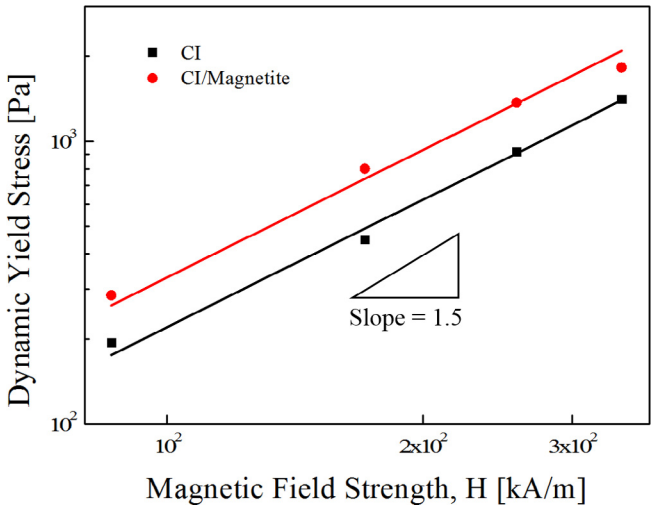

Fig. 3. Replotted dynamic yield stress versus magnetic field strengths for CI (30% wt) and CI/Magnetite (30%wt CI and 0.5%wt magnetite).

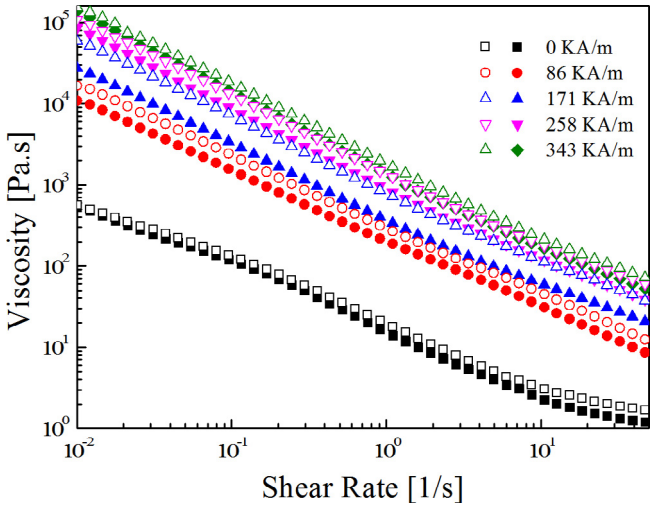

Fig. 4. Viscosity versus shear rate of pure CI (30%wt, closed) and CI/Magnetite (30% wt CI and 0.5%wt magnetite, open) under applying different magnetic field strength.

In Fig. 4, the shear thinning phenomena of the CI and CI/magnetite-based MR fluids was clearly observed because the shear viscosity decreased with increasing shear rate over the shear rate region examined [28]. Moreover, the shear viscosity of the CI/magnetite-based MR fluid was higher than that of the pure CI. Therefore, the shear viscosity, which is a major factor governing the MR properties, can be improved by adding magnetite nanoparticles. An increase in the MR properties by adding some magnetic particles to the MR suspension was also reported for -Fe_2O_3 [29], Ni-Zn ferrite [30], and Fe-MCM-22 [31]. In the absence of a magnetic field, the shear viscosity increased slightly with the addition of magnetite to the suspension, which is in good agreement with the literature regarding contractual additive MR-suspension systems [32].

To examine the ability to produce a solid-like structure, a frequency sweep test was performed at a fixed strain value, in which the suspension demonstrated linear viscoelastic (LVE) behavior. The LVE region was identified by an amplitude sweep test carried out at a fixed frequency of 6.28 rad/s under different magnetic field strengths. The storage modulus (G'), as a representative of the elastic portion of MR fluids, was determined as a function of strain. According to Fig. 5, in a low shear strain region, there was little relationship with strain but the storage modulus decreased stepwise when the strain was increased to more than the LVE region due to irreversible changes to the solid-like structure to a liquid-like structure. Hence, a liquid-like structure might be observed at a high range of strain. Therefore, a 0.02% strain was selected to ensure that deformation Occurred in the chain structure while performing the frequency sweep test. Both pure CI and CI/magnetite suspensions exhibited a saturation state at 171 kA/m, which

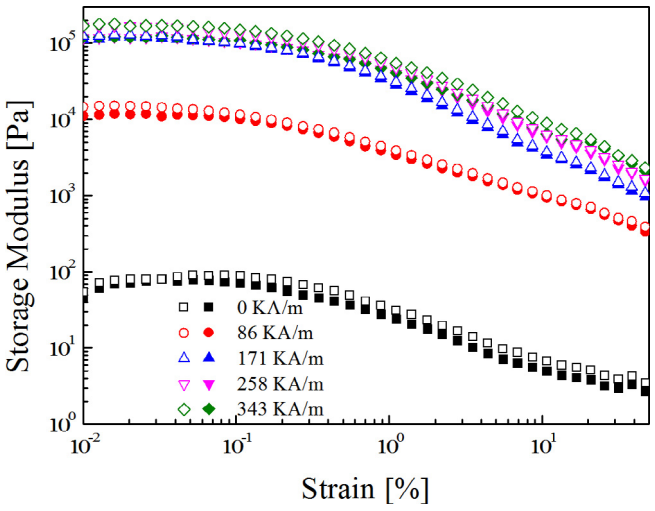

Fig. 5. Strain amplitude sweep test of pure CI (30%wt, closed) and CI/Magnetite (30%wt CI and 0.5%wt magnetite, open).

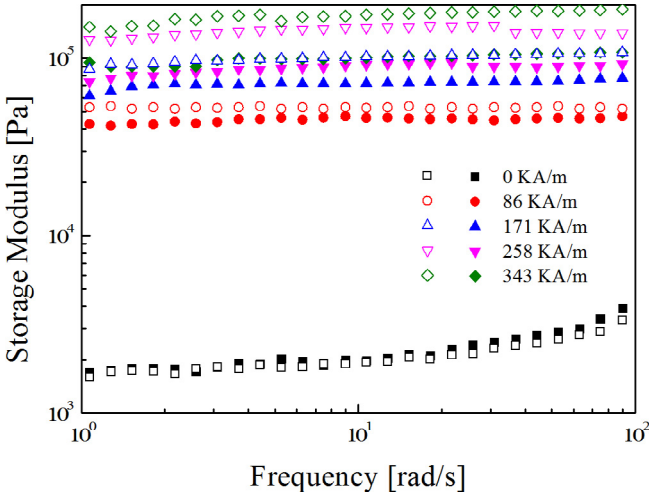

Fig. 6. Frequency sweep test of pure CI (30%wt, closed) and CI/Magnetite (30%wt CI and 0.5%wt magnetite, open).

explains why there were no significant changes above this magnetic field strength.

An angular frequency sweep test was conducted at a selected shear strain (0.02%) and according to Fig. 6, in the absence of a magnetic field, the elastic properties of both CI and CI/magnetite were fairly low and weak because in a high frequency region, the dynamic moduli were enhanced slightly. On the other hand, after applying the magnetic field, it retained a plateau region in the region of angular frequency from 1 rad/s to 100 rad/s along the enhancement of the magnetic field strength. The addition of magnetite nanoparticles to a CI suspension has a positive impact on boosting the elastic properties, irrespective of the magnetic field strength.

3.2. Experimental design

Through a wide variety of studies, some factors, such as CI, the additive amount in MR suspensions and the magnetic field strength, have a major impact on the MR response. MR tests were designed using a response surface methodology (RSM) to determine the effects of these factors and achieve a model for optimization or predicting the MR characteristics. The design optimumas one of the favorite RSM approaches was engaged. The RSM commonly establishes a functional relationship between the independent variables and response through two following models:

$$Y = \beta_0 + \sum_{i=1}^{k} \beta_i x_i \tag{5}$$

$$Y = \beta_0 + \sum_{i=1}^{k} \beta_i x_i + \sum \sum_{i<j} \beta_{ij} x_i x_j + \sum_{i=1}^{k} \beta_{ii} x_i^2 \tag{6}$$

where Y is the response, β_0 is a constant value, k is the number of inputs, β_i is a linear coefficient, x_i is a single factor, β_{ij} is an interaction or quadratic coefficient, and $x_i x_j$ is the interaction factor [33].

In this study, three control factors mentioned above were considered: the weight percentage of CI particles (from 30 to 70), weight percentage of additive particles (from 0 to 1), and magnetic field strength (86 to 343 KA/m). The yield stress and shear viscosity were the goal functions of the problem in the phrase of those factors. With a yield stress and shear viscosity, the shear stress can be calculated as a function of the shear rate using a Bingham fluid model. It can be also noted that the shear stress of the parallel plate

Table 2
Experimental design matrix with corresponding responses.

Std	Run	Factor 1 A: CI (%wt)	Factor 2 B: Additive (%wt)	Factor 3 C: Magnetic field Strength (KA/m)	Response 1 Yield Stress (Pa)	Response 2 Shear Viscosity (cP)
2	1	30	0	86	195	3.90
5	2	70	0.5	86	845	9.81
9	3	50	1	86	435	4387
4	4	50	0.5	86	552	5.8
1	5	30	1	343	1325	22.51
18	6	30	0	343	1407	19.08
8	7	70	0	86	896	9.76
7	8	70	0.5	343	7432	56.75
11	9	50	0.25	171	4334	37.13
20	10	30	0	86	194	3.90
14	11	70	1	343	7590	71.52
15	12	50	1	258	2613	30.33
3	13	70	0	343	7603	56.65
10	14	70	1	258	4729	56.65
12	15	30	1	86	244	4.20
6	16	50	0.5	343	3630	38.11
16	17	30	1	343	1343	21.7
13	18	70	1	86	908	11.22
19	19	70	0	86	896	9.76
17	20	70	0	343	7650	57.20

Table 3
Sequential models sum of squares.

Source	Response	Sum of Squares	df	Mean Square	F Value	p-value Prob > F
Mean vs Total	Yield Stress	9.982E + 007	1	9.982E + 007	–	–
	Shear Viscosity	9157.28	1	9157.28	–	–
Linear vs Mean	Yield Stress	1.007E + 008	3	3.355E + 007	23.03	<0.0001
	Shear Viscosity	6152.07	3	2050.69	29.55	<0.0001
2FI vs Linear	Yield Stress	1.804E + 007	3	6.013E + 006	66.57	<0.0001 suggested
	Shear Viscosity	750.46	3	250.15	16.48	0.0003
Quadratic vs 2FI	Yield Stress	2.847E + 005	3	94890.16	1.07	0.4198
	Shear Viscosity	143.24	3	47.75	39.07	<0.0001 suggested
Residual	Yield Stress	1237.27	4	309.32	–	–
	Shear Viscosity	2.00	4	0.50	–	–

Table 4
Model summary statistics.

Source	Response	SD	R^2	Adjusted R^2	Predicted R^2
Linear	Yield Stress	1207.09	0.84	0.80	0.71
	Shear Viscosity	8.33	0.87	0.84	0.77
2FI	Yield Stress	300.55	0.99	0.99	0.98
	Shear Viscosity	3.9	0.98	0.97	0.92
Quadratic	Yield Stress	297.28	0.99	0.98	0.91
	Shear Viscosity	1.11	0.99	0.99	0.98

is obtained by the machine, using a Newtonian fluid model in the shear stress calculation intrinsically. Table 2 lists the matrix of factors along with the corresponding yield stress and shear viscosity. Using a valid model, the best adjustment of factors could be determined by the RSM approach to obtain the optimal value of the corresponding response.

3.3. Fitting model for MR characteristics

To make expedient regression equations, a two-factor interaction (2FI), quadratic, and linear models were applied to analyze the experimental results. The following three distinct tests were performed to show the acceptability of the models depicting the MR characteristics (Table 3): a lack of fitting test, model summery results, and sequential model sum of squares. According to the p-value of the 2FI and quadratic model (Table 3) for the yield stress and shear viscosity, respectively, the Design Expert software found the models to be significant. Based on the model summery statistic (Table 4), R^2 was 0.99 for both models. Although R^2 quantifies the proportion of the variance described by a statistical model and a value close to unity indicates a perfect fit, it cannot quantify the model alone because R^2 always increases artificially when adding a new predictor [34]. To solve this problem, a modified form of R^2, which is called the adjusted R-square (R^2_{adj}) was used to assess the degree of relevance in the pivotal population because it increases when beneficial terms are embedded in the equation and decreases when pointless variables are added [35]; hence, it can assess a model more appropriately. The R^2_{adj} for both models was 0.99, showing that the regression of the models was powerful. The ability of the proposed models to predict the future observation was assessed using predicted R-squared (R^2_{pred}), which is equal to 0.98 for both models and is in reasonable agreement with the R^2_{adj} values. These three parameters proved the ability of both models for favorable fitness. Fig. 7 and Fig. 8 present the normal prob-

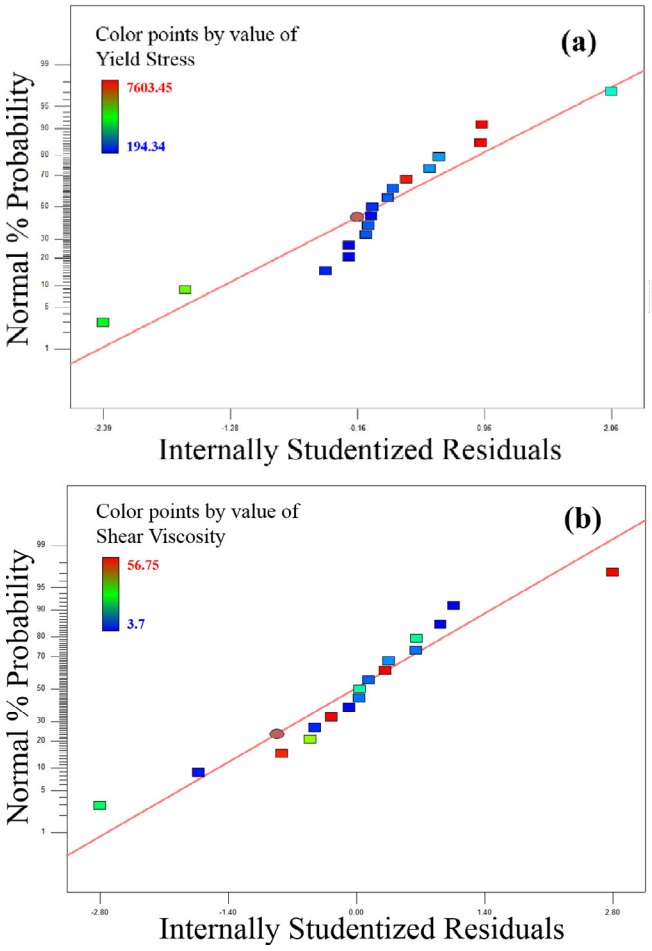

Fig. 7. Normal plot of residuals (a) for yield stress and (b) for shear viscosity.

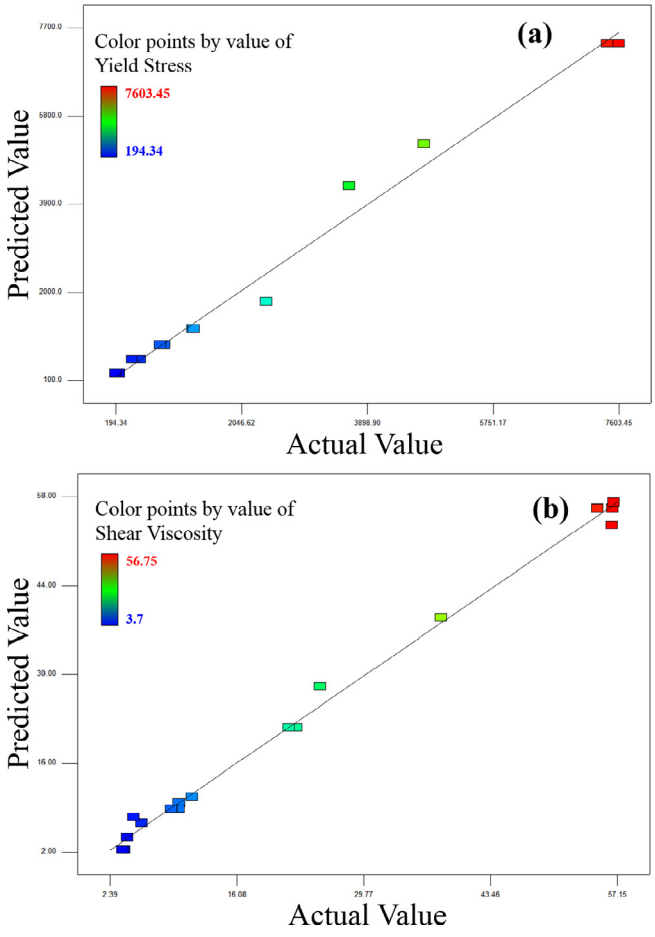

Fig. 8. Plot of actual and predicted values (a) for yield stress and (b) for shear viscosity.

ability plot, which displays the normal distribution of the residuals, and the correlation between the predicted and experimental value, respectively. The data points in Fig. 7 follow reasonably a straight line, highlighting the good fitness of both models. In Fig. 8, the predicted values were calculated using the proposed models. The data were scattered near a straight line, which shows proper agreement between the predicted and experimental values of the response.

Regression analysis was performed to fit the response as a function of the CI weight percentage (a), additive (magnetite) weight percentage (b), and magnetic field strength (c). Therefore, two empirical models between the input variables in the coded factors and responses are expressed as follows:

$$\text{Yield Stress} = 2427 + 1690a + 1865c + 1383ac \quad (7)$$

$$\text{Shear Viscosity} = 35.3 + 10.7a + b + 16.2c + 7.5ac - 12.6c^2 \quad (8)$$

These are the reduced-order equations because unnecessary (insignificant) terms were removed from the model. Having these two models, the yield stress and shear viscosity could be predicted properly in the range of factors and there was no need to conduct an experiment. Another unique aspect of this model is that the amount of CI or additive or magnetic field strength can be determined based on the favorite yield stress and shear viscosity. Moreover, the optimization process can be performed when a certain value of responses are required. On the other hand, it can be also noted that Sidpara et al. [36] applied response surface methodology to study effect of volume concentration of each component in MR fluids by conducting analysis of variance with non-magnetic silica particles as an additive.

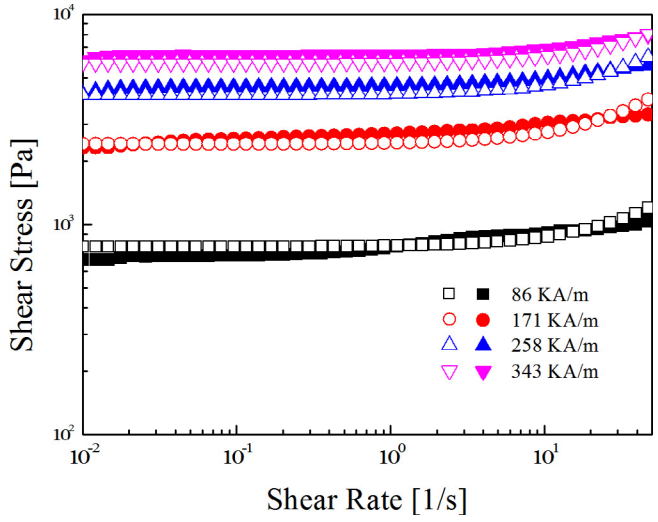

Fig. 9. Shear stress versus shear rate of CI/Magnetite (60 wt%/0.25%wt), predicted values by model (open) and data from experiment (close) under applying different magnetic field strength.

3.4. Model validation

Although the discussed parameters, such as R^2, R^2_{adj} and R^2_{pred}, and Fig. 7 and Fig. 8), show that the proposed models can predict the MR characteristic appropriately, this is the first report of a model based on the weight percentage of magnetic particles. Therefore, the model was validated. To compare the calculated MR behavior by models and experimental results, a new sample was selected randomly and prepared with 60 wt% CI and 0.25 wt% additive (magnetite) in silicon oil. A controlled shear rate mode at 4 magnetic fields strengths (from 86 to 343 KA/m) was applied to examine the shear stress as a function of the shear rate. The data of this sample was not embedded to produce models and this is a new sample in the range of the discussed input factors. As shown in Fig. 9, there is a good match between the predicted results and actual data, which confirm the ability of the proposed model.

4. Conclusion

The MR characteristics of a pure CI and CI/Magnetite suspension were investigated by rotation rheometry under different magnetic field strengths. The results were fitted to the Bingham, Herschel-Bulkley and Casson model. The MR properties of CI/Magnetite increase slightly due to the addition of magnetite, and it was confirmed that both systems could produce a solid-like structure in a magnetic field. Furthermore, using the analysis of the variance technique, the yield stress and shear viscosity were modeled based on the CI wt.%, additive (magnetite) wt.% and magnetic field strength. The 2FI and quadratic models were fitted to the yield stress and shear viscosity, respectively, and high adequacy equations were obtained for both. The validity of the models were confirmed by statistical parameters, such as R^2, R^2_{adj}, and R^2_{pred}, as well as the normal plot residual and prediction plot. A double check validation was also performed on a sample that had not been used for modeling and a good match was found. The proposed models can predict the MR response of CI suspensions properly and can be used with high accuracy in all aspects of application, particularly in industry.

Acknowledgements

One of authors (HJC) was partially supported by the Ministry of Trade, Industry & Energy, Korea (#10047791). The authors are

thankful to Stat-Ease, Minneapolis for the provision of the Design Expert package.

References

[1] G. Wang, Y. Ma, Y. Tong, X. Dong, Development of manganese ferrite/graphene oxide nan Composites for magnetorheological fluid with enhanced sedimentation stability, J. Ind. Eng. Chem. 48 (2017) 142–150.

[2] I. Bica, Electrical conductivity of magnetorheological suspensions based on iron microparticles and mineral oil in alternative magnetic field, J. Ind. Eng. Chem. 12 (2006) 806–810.

[3] D. Susan-Resiga, L. Vékás, Yield stress and flow behavior of concentrated ferrofluid-based magnetorheological fluids: the influence of composition, Rheol. Acta 53 (2014) 645–653.

[4] K. Chung, U. Jeong, J.E. Oh, Effects of magnetic field input cycle and peptizer on the MR effect of magneto-rheological elastomer based on natural rubber, Polym. Eng. Sci. 55 (2015) 2669–2675.

[5] I. Bica, Y.D. Liu, H.J. Choi, Physical characteristics of magnetorheological suspensions and their applications, J. Ind. Eng. Chem. 19 (2013) 394–406.

[6] A. Sidpara, V.K. Jain, Rheological properties and their correlation with surface finish quality in MR fluid-based finishing process, Machining Sci. Tech. 18 (2014) 367–385.

[7] G.R. Iglesias, A. Roldán, L. Reyes, L. Rodríguez-Arco, J.D. Durán, Stability behavior of composite magnetorheological fluids by an induction method, J. Intell. Mater. Sys. Struct. 26 (2015) 1836–1843.

[8] I.D. Jung, M. Kim, S.J. Park, A comprehensive viscosity model for micro magnetic particle dispersed in silicone oil, J. Magn. Magn. Mater. 404 (2016) 40–44.

[9] W. Guangshuo, M. Yingying, T. Yu, D. Xufeng, Synthesis, characterization and magnetorheological study of 3-aminopropyltriethoxysilane-modified Fe_3O_4 nanoparticles, Smart Mater. Struct. 25 (2016) 035028.

[10] J. Yang, H. Yan, X. Wang, Z. Hu, Enhanced yield stress of magnetorheological fluids with dimer acid, Mater. Lett. 167 (2016) 27–29.

[11] L. Shan, W. Jia, M. Zhou, Y. Meng, X. Zhang, Y. Tian, Frequency-independent viscoelasticity of carbonyl iron particle suspensions under a magnetic field, Smart Mater. Struct. 26 (2017) 054009.

[12] X. Ruan, L. Pei, S. Xuan, Q. Yan, X. Gong, The rheological responds of the superparamagnetic fluid based on Fe_3O_4 hollow nanospheres, J. Magn. Magn. Mater. 429 (2017) 1–10.

[13] E. Ghasemi, A. Mirhabibi, M. Edrissi, Magneto viscous effect in a maghemite ferrofluid, J. Nanosci. Nanotech. 11 (2011) 5285–5291.

[14] A.J.F. Bombard, M. Knobel, M.R. Alcantara, I. Joekes, Evaluation of magnetorheological suspensions based on carbonyl iron powders, J. Intel. Mater. Sys. Struct. 13 (2002) 471–478.

[15] M. Cvek, M. Mrlik, V. Pavlinek, A rheological evaluation of steady shear magnetorheological flow behavior using three-parameter viscoplastic models, J. Rheol. 60 (2016) 687–694.

[16] G.R. Iglesias, M.T. López-López, J.D.G. Durán, F. González-Caballero, A.V. Delgado, Dynamic characterization of extremely bidisperse magnetorheological fluids, J. Colloid Interf. Sci. 377 (2012) 153–159.

[17] D.H. Bae, H.J. Choi, K. Choi, J.D. Nam, M.S. Islam, N. Kao, Micr Crystalline cellulose added carbonyl iron suspension and its magnetorheology, Colloids Surf. A: Physic Chem. Eng. Asp. 514 (2017) 161–167.

[18] F.F. Fang, H.J. Choi, M.S. Jhon, Magnetorheology of soft magnetic carbonyl iron suspension with single-walled carbon nanotube additive and its yield stress scaling function, Colloids Surf. A: Physic Chem. Eng. Asp. 351 (2009) 46–51.

[19] M.T. Lopez-Lopez, J. de Vicente, F. Gonzalez-Caballero, J.D.G. Duran, Stability of magnetizable colloidal suspensions by addition of oleic acid and silica nanoparticles, Colloids Surf. A: Physic Chem. Eng. Asp. 264 (2005) 75–81.

[20] J.P. Rich, P.S. Doyle, G.H. McKinley, Magnetorheology in an aging, yield stress matrix fluid, Rheol. Acta 51 (2012) 579–593.

[21] W.L. Zhang, S.D. Kim, H.J. Choi, Effect of graphene oxide on carbonyl-iron-based magnetorheological fluid, IEEE Trans. Magn. 50 (2014) 1–4.

[22] S. Vinod, R. John, J. Philip, Magnetorheological properties of sodium sulphonate capped electrolytic iron based MR fluid: a comparison with CI based MR fluid, Smart Mater. Struct. 26 (2016) 025003.

[23] C. Hui, C. Shen, T. Yang, L. Bao, J. Tian, H. Ding, C. Li, H.-J. Gao, Large-scale Fe_3O_4 nanoparticles soluble in water synthesized by a facile method, J. Phys. Chem. C 112 (2008) 11336–11339.

[24] N. Wereley, A. Chaudhuri, J.-H. Yoo, S. John, S. Kotha, A. Suggs, R. Radhakrishnan, B. Love, T. Sudarshan, Bidisperse magnetorheological fluids using Fe particles at nanometer and micron scale, J. Intell. Mater. Syst. 17 (2006) 393–401.

[25] I. Kim, K. Song, B. Park, B. Choi, H.J. Choi, Nano-sized Fe soft-magnetic particle and its magnetorheology, Colloid Polym. Sci. 289 (2011) 79–83.

[26] R. Bell, J. Karli, A. Vavreck, D. Zimmerman, G. Ngatu, N. Wereley, Magnetorheology of submicron diameter iron microwires dispersed in silicone oil, Smart Mater. Struct. 17 (2008) 015028.

[27] F.F. Fang, Y.D. Liu, H.J. Choi, Carbon nanotube coated magnetic carbonyl iron microspheres prepared by solvent casting method and their magneto-responsive characteristics, Colloids Surf. A 412 (2012) 47–56.

[28] M.G. Jang, Y.K. Lee, W.N. Kim, Influence of lactic acid-grafted multi-walled carbon nanotube (LA-*g*-MWCNT) on the electrical and rheological properties of polycarbonate/poly(lactic acid)/LA-*g*-MWCNT composites, Macromol. Res. 23 (2015) 916–923.

[29] D.S. Jang, Y.D. Liu, J.H. Kim, H.J. Choi, Enhanced magnetorheology of soft magnetic carbonyl iron suspension with hard magnetic γ-Fe_2O_3 nanoparticle additive, Colloid Polym. Sci. 293 (2015) 641–647.

[30] A. Hajalilou, S.A. Mazlan, S.T. Shila, Magnetic carbonyl iron suspension with Ni-Zn ferrite additive and its magnetorheological properties, Mater. Lett. 181 (2016) 196–199.

[31] X.M. Quan, Y.D. Liu, W.-S. Ahn, H.J. Choi, Nanoporous Fe-MCM-22 additive effect on magnetorheological response of magnetic carbonyl iron suspension, IEEE Trans. Magn. 49 (2013) 3410–3413.

[32] M.J. Hato, H.J. Choi, H.H. Sim, B.O. Park, S.S. Ray, Magnetic carbonyl iron suspension with organ Clay additive and its magnetorheological properties, Colloids Surf. A 377 (2011) 103–109.

[33] A.I. Khuri, S. Mukhopadhyay, Response surface methodology, Wiley Interdiscip Rev Comput Stat 2 (2010) 128–149.

[34] A. Lo, H. Chernoff, T. Zheng, S.-H. Lo, Why significant variables aren't automatically good predictors, Proc. Natl. Acad. Sci. 112 (2015) 13892–13897.

[35] J.M. Wooldridge, A note on computing r-squared and adjusted r-squared for trending and seasonal data, Econ. Lett. 36 (1991) 49–54.

[36] A. Sidpara, M. Das, V.K. Jain, Rheological characterization of magnetorheological finishing fluid, Mater. Manufac. Process. 24 (2009) 1467–1478.